

as wetting or adhesion (14), and fabrication of microelectromechanical systems (15) and sensors (16).

REFERENCES AND NOTES

1. M. C. Hutley, *Diffraction Gratings* (Academic Press, New York, 1982).
2. H. C. Haverkorn van Rijsewijk, P. E. J. Legierse, G. E. Thomas, *Phillips Tech. Rev.* **40**, 287 (1982); H. W. Lehmann, R. Widmer, M. Ebnoether, *J. Vac. Sci. Technol. B* **1** (no. 4), 1207 (1983).
3. S. J. Clarson and J. A. Semlyen, Eds., *Siloxane Polymers* (PTR Prentice Hall, Englewood Cliffs, NJ, 1993).
4. Y. Xia and G. M. Whitesides, *Adv. Mater.* **7**, 471 (1995).
5. A. Kumar and G. M. Whitesides, *Appl. Phys. Lett.* **63**, 2002 (1993); Y. Xia, M. Mrksich, E. Kim, G. M. Whitesides, *J. Am. Chem. Soc.* **117**, 9576 (1995); Y. Xia, E. Kim, G. M. Whitesides, *J. Electrochem. Soc.* **143**, 1070 (1996); Y. Xia, E. Kim, M. Mrksich, G. M. Whitesides, *Chem. Mater.* **8**, 601 (1996).
6. Sylgard 184 (Dow Corning, A:B = 1:20) silicone elastomer was used. It was cured at room temperature for ~2 hours and then at ~65°C for ~6 hours. Ultraviolet-curable PU (NOA-73; Norland Products, New Brunswick, NJ) was cured with a medium-pressure mercury vapor lamp (450 W, ACE Glass, Louisville, KY) for ~20 min, with the lamp positioned ~2 cm from the sample. Blazed gratings were obtained from Edmund Scientific.
7. Computer simulation was done with PDEase2, Finite Element Analysis for Partial Differential Equations, version 2.5.2.
8. A. C. Livanos, A. Katzir, A. Yariv, *Opt. Commun.* **20**, 179 (1976); W. M. Gibsons and S.-T. Sun, *Appl. Phys. Lett.* **65**, 2542 (1994).
9. This different behavior can be attributed to their difference in period. When a blazed grating is used in transmission, each groove acts as a prism, and the condition for blazing is given by  $\Lambda \tan \phi [n - (1 - \lambda^2/d^2)^{1/2}] = \lambda (1)$ , where  $\Lambda$  is the period of the grating,  $n$  is the refractive index of the grating material, and  $\phi$  is the facet angle. The PDMS master replicated from the commercial grating blazes in the near-infrared region (~1000 nm); the chirped grating is expected to blaze at shorter wavelengths (that is, closer to the wavelength of the visible laser that was used) because the period of the chirped grating is shorter than that of the PDMS master. The relation between the diffraction angle  $\theta$  and  $z$  can be described by  $\theta = \sin^{-1}[\lambda(zd/\Lambda dz + \Lambda_0)]$ , where  $\Lambda_0$  is the period at  $z = 0$ ; the diffraction angles so calculated were in agreement with the measured values.
10. PDMS prepolymer reaction mixture (Sylgard 184, A:B = 1:15) about 1 mm thick was poured over a rigid master that was placed in a plastic petri dish. The PDMS was cured in an oven for ~5 hours at ~65°C. A glass tube (~4 cm long) was then vertically placed on the top of the cured PDMS, and PDMS prepolymer reaction mixture (A:B = 1:10) ~0.5 cm thick was added. The glass tube was pressed against the first layer of PDMS with Scotch tape, and no fresh PDMS prepolymer reaction mixture could enter the glass tube. The whole system was cured at room temperature for ~12 hours and then at ~65°C for ~5 hours. Adhesion between the second layer of PDMS and the glass was good.
11. The master was fabricated according to a three-stage procedure (5, 12): (i) the first used microcontact printing to form lines of hexadecanethiolate on a silver surface; (ii) the second used microcontact printing to print lines of hexadecanethiolate perpendicular to the lines of (i) on the same silver surface; (iii) the third assembled liquid prepolymer reaction mixture of PU onto the bare regions of the silver surface and cured the liquid PU under an ultraviolet light.
12. H. A. Biebuyck and G. M. Whitesides, *Langmuir* **10**, 2790 (1994).
13. R. Singhvi et al., *Science* **264**, 696 (1994); P. Clark et al., *Development* **108**, 635 (1990).
14. L.-H. Lee, Ed., *Fundamentals of Adhesion* (Plenum, New York, 1991).
15. J. Bryzek, K. Petersen, W. McCulley, *IEEE Spec-*

trum (May 1994), p. 20.

16. R. C. Hughes, A. J. Ricco, M. A. Butler, S. J. Martin, *Science* **254**, 74 (1991); K. D. Wise and K. Najafi, *ibid.*, p. 1335; J. Heinze, *Angew. Chem. Int. Ed. Engl.* **32**, 1268 (1993).
17. Supported in part by the Office of Naval Research, the Advanced Research Projects Agency, and the National Science Foundation (NSF) (PHY 9312572). This work

made use of Materials Research Science and Engineering Center Shared Facilities supported by NSF (grant DMR-9400396). The work of J.A.R. was supported by the Harvard University Society of Fellows. We thank Y. Lu and S. Shepard for assistance with SEM and photolithographic instruments.

4 March 1996; accepted 3 June 1996

## Cytoplasmic Tail-Dependent Localization of CD1b Antigen-Presenting Molecules to MIICs

Masahiko Sugita, Robin M. Jackman, Elly van Donselaar, Samuel M. Behar, Rick A. Rogers, Peter J. Peters, Michael B. Brenner, Steven A. Porcelli\*

CD1 proteins have been implicated as antigen-presenting molecules for T cell-mediated immune responses, but their intracellular localization and trafficking remain uncharacterized. CD1b, a member of this family that presents microbial lipid antigens of exogenous origin, was found to localize to endocytic compartments that included the same specialized subset of endosomes in which major histocompatibility complex (MHC) class II molecules are proposed to bind endocytosed antigens. Unlike MHC class II molecules, which traffic to antigen-loading endosomal compartments [MHC class II compartments (MIICs)] primarily as a consequence of their association with the invariant chain, localization of CD1b to these compartments was dependent on a tyrosine-based motif in its own cytoplasmic tail.

Non-MHC encoded CD1 molecules have been implicated as a family of  $\beta_2$ -microglobulin-associated nonpolymorphic polypeptides that function in antigen presentation. Identification of a T cell line that recognizes mycolic acid, a complex fatty acid from the mycobacterial cell wall, in a CD1b-restricted fashion (1) and the subsequent derivation of two other CD1b-restricted T cell lines that recognize lipoarabinomannan from *Mycobacterium leprae* demonstrate the capability of CD1b to present exogenously derived microbial lipid antigens (2). These CD1b-restricted lipid and glycolipid antigens appear to require intracellular processing in acidic compartments, as do peptide antigens presented by MHC class II molecules (1, 2). Thus, it is proposed that CD1b molecules, despite their MHC class I-like protein structure (3), might traffic to endocytic compartments, including those in which MHC class II molecules encounter endocytosed antigens.

As was consistent with this hypothesis, CD1b induced on peripheral blood monocytes by stimulation with granulocyte-macrophage colony-stimulating factor (GM-CSF) and in-

terleukin-4 (IL-4) (1) was found by immunofluorescence microscopy not only on the cell surface, but also in peripherally distributed vesicles into which Texas Red-conjugated ovalbumin was endocytosed (Fig. 1). Double labeling of CD1b<sup>+</sup> monocytes with antibodies against lysosome-associated membrane protein 1 (LAMP-1, a marker of late endosomes and lysosomes) showed that most CD1b<sup>+</sup> endocytic vesicles coexpressed this protein (4). Furthermore, most CD1b<sup>+</sup> vesicles in monocytes, as well as in a CD1b-transfected human B cell line (C1R/CD1b) (1) stained with antibodies to MHC class II molecules (4). This profile was characteristic of the recently described MHC class II compartment (MIIC) of specialized or "professional" antigen-presenting cells, which is the proposed site at which newly synthesized MHC class II molecules accumulate and acquire exogenous peptide antigens (5-7).

Previous studies using electron microscopy have identified MIICs morphologically as electron-dense structures, characterized by extensive membrane invaginations producing either a multivesicular or multilamellar appearance (5-7). Immunogold-labeled transmission electron microscopy of ultrathin cryosections of GM-CSF- and IL-4-stimulated monocytes revealed expression of CD1b in MHC class II-positive dense multilamellar organelles (Fig. 2A), which were characteristic of MIICs previously observed in mononuclear phagocytes (8). As was consistent with the localization of CD1b in

M. Sugita, R. M. Jackman, S. M. Behar, M. B. Brenner, S. A. Porcelli, Lymphocyte Biology Section, Division of Rheumatology and Immunology, Brigham and Women's Hospital, Harvard Medical School, Boston, MA 02115, USA. E. van Donselaar and P. J. Peters, Department of Cell Biology and Institute of Biomembranes, Faculty of Medicine, University of Utrecht, Utrecht, Netherlands. R. A. Rogers, Department of Environmental Health, Harvard School of Public Health, Boston, MA 02115, USA.

\*To whom correspondence should be addressed.

MIICs, these CD1b<sup>+</sup> multilamellar compartments were also positive for LAMP-1 (9) and for human leukocyte antigen DM (HLA-DM) (Fig. 2B), which has been found to be mainly expressed in MIICs in human cells (7). CD1b was also found to be strongly colocalized with MHC class II molecules by immunogold labeling in electron-dense multivesicular compartments of C1R/CD1b cells (Fig. 2E). These compartments were also positive for HLA-DM and LAMP-1 (9) and were morphologically consistent with MIICs previously defined in human B cell lines (5).

In addition, CD1b was found in plasma membrane-coated pits and coated vesicles and in early endosomes in CD1b<sup>+</sup> monocytes and C1R/CD1b cells (Fig. 2, C through E). Despite the coexpression of CD1b and MHC

class II molecules on the cell surface, these CD1b<sup>+</sup> coated vesicles and early endosomes lacked coexpression of MHC class II molecules (Fig. 2, D and E), which suggests a much more pronounced internalization from the cell surface for CD1b than for MHC class II molecules. These observations led us to focus on the role of the cytoplasmic domain of CD1b in its localization to endocytic compartments, as the amino acid sequence of this domain (Met-Arg-Arg-Arg-Ser-Tyr-Gln-Asn-Ile-Pro) contains a YXXZ sequence (Y, tyrosine; X, any amino acid; and Z, a hydrophobic amino acid; the sequence corresponding to the motif is in italics) (10). This motif has been identified in many proteins that are predominantly found in the endocytic system and is known to cause rapid internalization of proteins from the cell surface (11, 12) as well

as direct targeting to endosomes from the trans-Golgi network (TGN) (13). Thus, we deleted the COOH-terminal seven amino acids, including the tyrosine-based motif, leaving a stretch of two basic amino acids to confer stable membrane insertion (14). An antibody internalization assay (15) with HeLa transfectant cells stably expressing either wild-type CD1b [full-length CD1b (CD1b-FL)] or truncated CD1b [tail-deleted CD1b (CD1b-TD)] showed that almost all the antibody-labeled CD1b-FL molecules on the cell surface were internalized during the 45-min chase period, whereas a substantial fraction of labeled CD1b-TD molecules remained on the cell surface even after the chase period, as indicated by the clear visualization of the edges of cells (Fig. 3A). Thus, truncation of the cytoplasmic tail with deletion of the tyrosine-based motif resulted in impaired internalization of CD1b from the cell surface.

We also observed a difference between CD1b-FL and CD1b-TD in steady-state intracellular localization. As shown in CD1b<sup>+</sup> monocytes (Fig. 1) and in HeLa transfectants (Fig. 3B, left), CD1b-FL was prominent in peripherally distributed vesicles. In contrast, labeling of permeabilized HeLa cells expressing CD1b-TD with antibody to CD1b revealed homogenous staining over the cell that is characteristic of strong cell-surface staining, with a small amount of visible punctate staining confined to the central part of the cell (Fig. 3B,

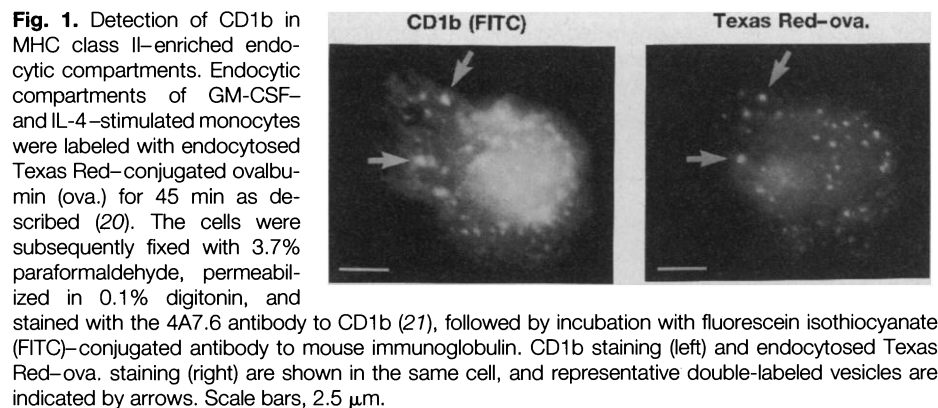


**Fig. 1.** Detection of CD1b in MHC class II-enriched endocytic compartments. Endocytic compartments of GM-CSF- and IL-4-stimulated monocytes were labeled with endocytosed Texas Red-conjugated ovalbumin (ova.) for 45 min as described (20). The cells were subsequently fixed with 3.7% paraformaldehyde, permeabilized in 0.1% digitonin, and stained with the 4A7.6 antibody to CD1b (21), followed by incubation with fluorescein isothiocyanate (FITC)-conjugated antibody to mouse immunoglobulin. CD1b staining (left) and endocytosed Texas Red-ova. staining (right) are shown in the same cell, and representative double-labeled vesicles are indicated by arrows. Scale bars, 2.5  $\mu$ m.

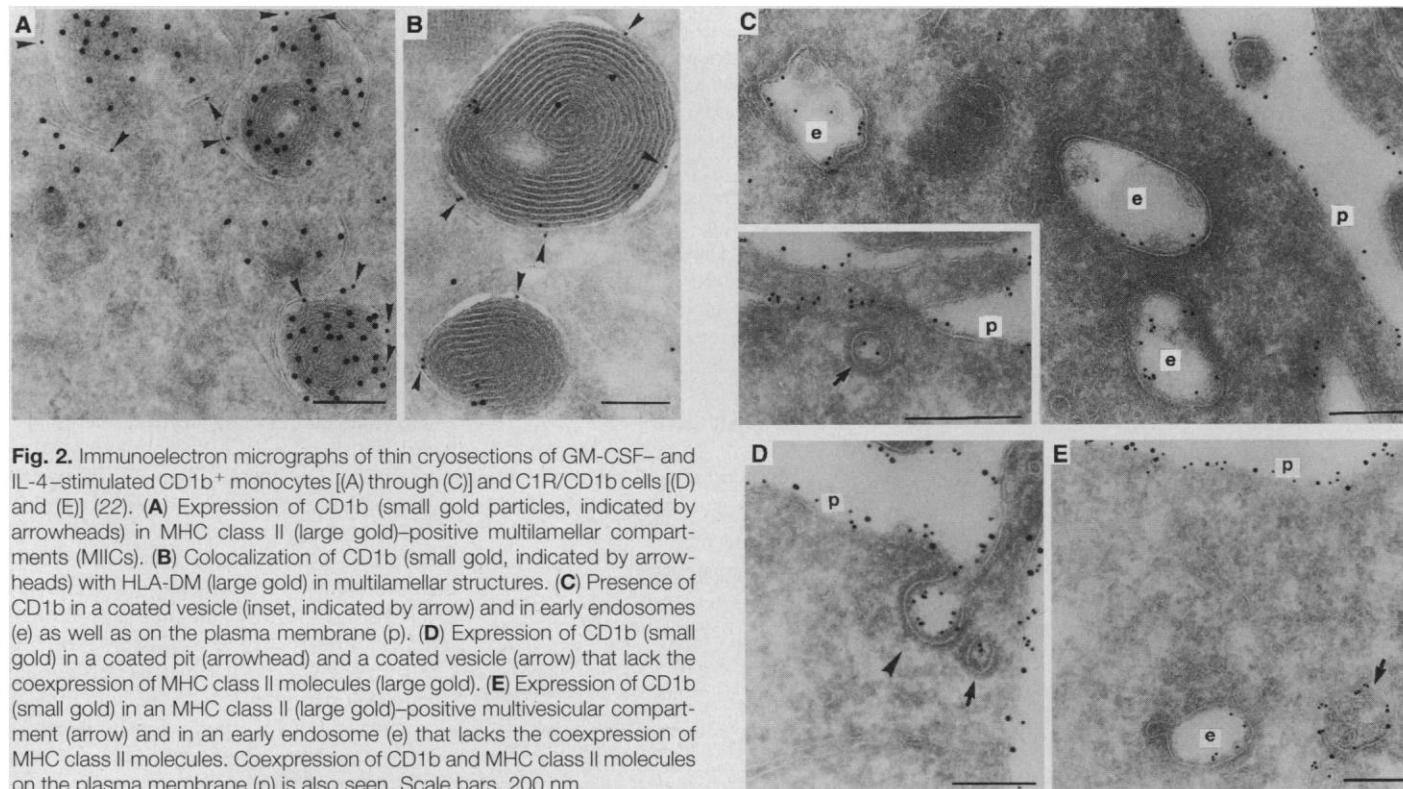


**Fig. 2.** Immunoelectron micrographs of thin cryosections of GM-CSF- and IL-4-stimulated CD1b<sup>+</sup> monocytes [(A) through (C)] and C1R/CD1b cells [(D) and (E)] (22). **(A)** Expression of CD1b (small gold particles, indicated by arrowheads) in MHC class II (large gold)-positive multilamellar compartments (MIICs). **(B)** Colocalization of CD1b (small gold, indicated by arrowheads) with HLA-DM (large gold) in multilamellar structures. **(C)** Presence of CD1b in a coated vesicle (inset, indicated by arrow) and in early endosomes (e) as well as on the plasma membrane (p). **(D)** Expression of CD1b (small gold) in a coated pit (arrowhead) and a coated vesicle (arrow) that lack the coexpression of MHC class II molecules (large gold). **(E)** Expression of CD1b (small gold) in an MHC class II (large gold)-positive multivesicular compartment (arrow) and in an early endosome (e) that lacks the coexpression of MHC class II molecules. Coexpression of CD1b and MHC class II molecules on the plasma membrane (p) is also seen. Scale bars, 200 nm.

right). These centrally located vesicles were identified as terminal lysosomes (4) to which proteins are generally transported via degradative pathways. Thus, without the influence of its cytoplasmic tail, CD1b was largely redistributed from the endocytic system to the plasma membrane.

Because the strong plasma-membrane CD1b staining of the CD1b-TD transfectants may have masked a substantial amount of intracellular staining, we used confocal microscopy (16) to examine the intracellular distribution of the full-length and tail-deleted forms of CD1b in optical sections of transfected HeLa cells. Cells expressing either CD1b-FL or CD1b-TD were supertransfected with HLA-DM $\alpha$  and -DM $\beta$ , and double labeling with antibodies to CD1b and HLA-DM was performed. HLA-DM was found in numerous peripherally distributed vesicles in both CD1b-FL-expressing and CD1b-TD-expressing cells (green vesicles in Fig. 4, B and E). However, whereas most of the CD1b-FL-expressing vesicles (red vesicles in Fig. 4A) were observed to coexpress HLA-DM (yellow vesicles in Fig. 4C), CD1b-TD was found intracellularly only in a relatively small number of vesicles at the central part of the cell (red vesicles in Fig. 4D; also see Fig. 3B, right). Colocalization analysis with HLA-DM revealed that only a limited number of CD1b-TD<sup>+</sup> vesicles coexpressed HLA-DM (yellow vesicles in Fig. 4F), whereas most peripherally distributed vesicles expressed HLA-DM alone (green vesicles in Fig. 4F), and some centrally distributed vesicles expressed CD1b alone (red vesicles in Fig. 4F). Thus, the cytoplasmic domain of CD1b markedly enhanced its localization in transfected HeLa cells to the same intracellular compartments as HLA-DM, a molecule that is expressed almost exclusively in the MIICs of professional antigen-presenting cells (7, 11). Although these studies identify the tyrosine-based motif as impor-

tant to the intracellular trafficking of CD1b, further studies will be needed to determine if this signal is by itself sufficient to direct endocytic localization or if other signals also contribute.

Trafficking of HLA-DM to MIICs has recently been shown to be mediated by a tyrosine-based motif in the cytoplasmic domain of HLA-DM $\beta$  (11) that is similar to that in the cytoplasmic domain of CD1b, as is consistent with the proposed role of this motif in the trafficking of CD1b to MIICs. In addition, the prominent localization of CD1b in coated pits (Fig. 2, C and D) underscored the role of the YXXZ motif in internalization of CD1b into the endocytic system, because this motif has been shown to mediate interaction with clathrin-associated protein complexes (17). Although the predominant route taken by

CD1b to the MIIC has not yet been defined, our results suggest a YXXZ motif-mediated recycling pathway by which CD1b is endocytosed at the plasma membrane and subsequently delivered to the MIIC. The use of such a pathway may be crucial for CD1b, whose de novo synthesis appears to be slower than that of MHC molecules (3, 18). The YXXZ sequence is found in neither MHC class II  $\alpha$  nor  $\beta$  chains, whose trafficking to MIICs is predominantly mediated by other sequences within the associated invariant chain that specify sorting of MHC class II molecules from the TGN to endocytic compartments (19). Thus, we propose that the targeting of CD1b to MIICs by a YXXZ cytoplasmic tail motif is a mechanism for controlling the intracellular trafficking and distribution of an antigen-presenting molecule.

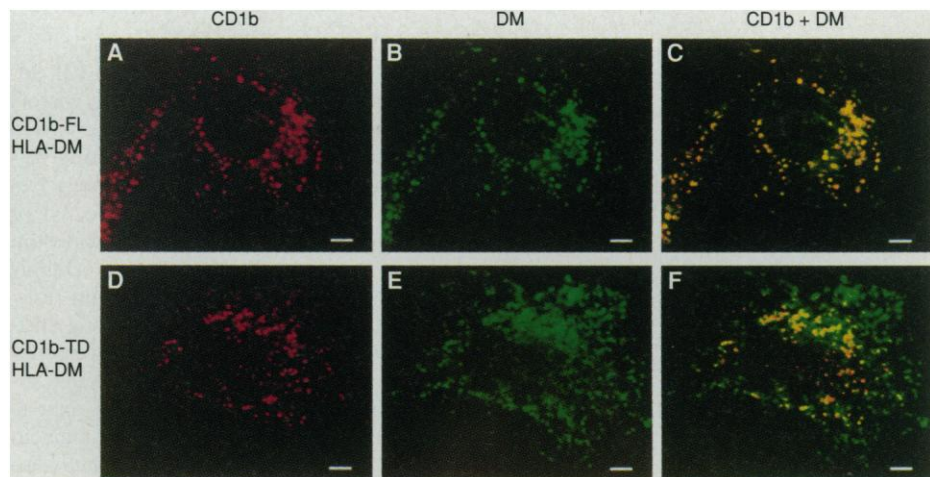


**Fig. 4.** Cytoplasmic tail-mediated transport of CD1b to HLA-DM-containing vesicles. HeLa CD1b-FL cells (upper panels) and HeLa CD1b-TD cells (lower panels) were transiently transfected with HLA-DM $\alpha$  and -DM $\beta$  (23), and double labeling with the 4A7.6 antibody [detected with indocarbocyanine-conjugated goat anti-mouse IgG (red)] and antibody to HLA-DM $\beta$  [detected with FITC-conjugated goat anti-rabbit IgG (green)] (23) was performed. Fluorescent confocal images of either CD1b-FL<sup>+</sup> (A) or CD1b-TD<sup>+</sup> (D) vesicles (red) and HLA-DM<sup>+</sup> vesicles (green) (B and E), as well as vesicles expressing both CD1b and HLA-DM (yellow) (C and F) are shown. Scale bars, 5  $\mu$ m.

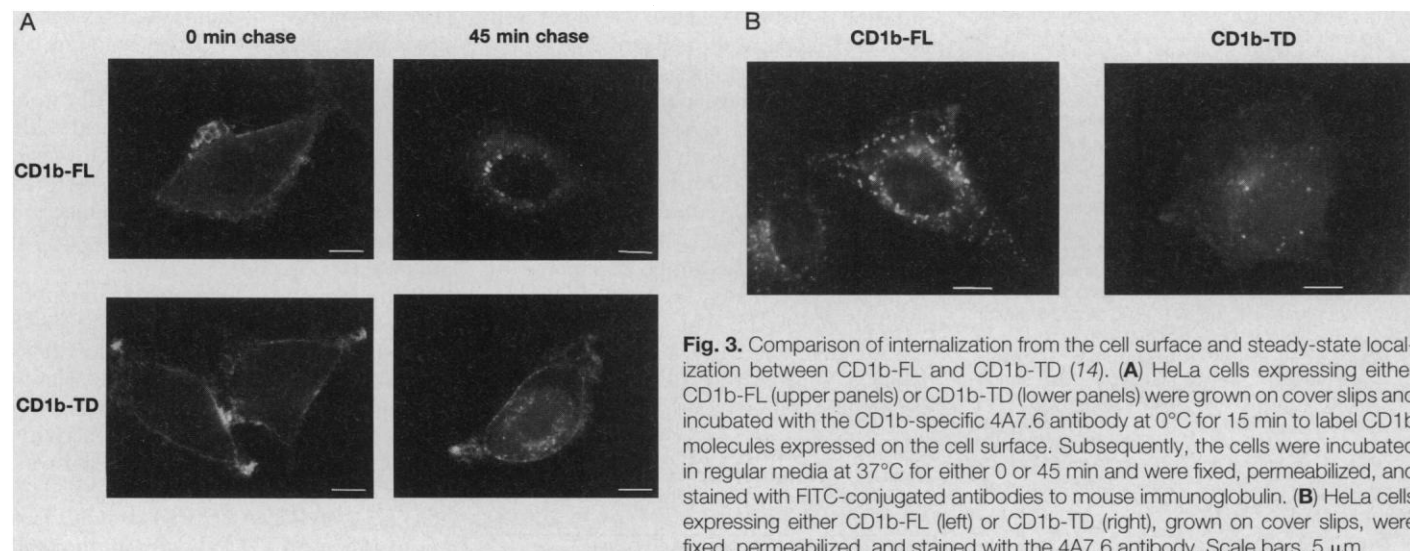


**Fig. 3.** Comparison of internalization from the cell surface and steady-state localization between CD1b-FL and CD1b-TD (14). (A) HeLa cells expressing either CD1b-FL (upper panels) or CD1b-TD (lower panels) were grown on cover slips and incubated with the CD1b-specific 4A7.6 antibody at 0°C for 15 min to label CD1b molecules expressed on the cell surface. Subsequently, the cells were incubated in regular media at 37°C for either 0 or 45 min and were fixed, permeabilized, and stained with FITC-conjugated antibodies to mouse immunoglobulin. (B) HeLa cells expressing either CD1b-FL (left) or CD1b-TD (right), grown on cover slips, were fixed, permeabilized, and stained with the 4A7.6 antibody. Scale bars, 5  $\mu$ m.

## REFERENCES AND NOTES

1. S. Porcelli *et al.*, *Nature* **341**, 447 (1989); S. Porcelli, C. T. Morita, M. B. Brenner, *ibid.* **360**, 593 (1992); E. M. Beckman *et al.*, *ibid.* **372**, 691 (1994).
2. P. A. Sieling *et al.*, *Science* **269**, 227 (1995); A. Bendelac, *ibid.*, p. 185.
3. S. A. Porcelli, *Adv. Immunol.* **59**, 1 (1995).
4. M. Sugita, unpublished observations.
5. P. J. Peters, J. J. Neefjes, V. Oorschot, H. L. Ploegh, H. J. Geuze, *Nature* **349**, 669 (1991); P. J. Peters *et al.*, *J. Exp. Med.* **182**, 325 (1995).
6. A. Tulp, D. Verwoerd, B. Dobberstein, H. L. Ploegh, J. Pieters, *Nature* **369**, 120 (1994).
7. F. Sanderson *et al.*, *Science* **266**, 1566 (1994).
8. H. W. Nijman *et al.*, *J. Exp. Med.* **182**, 163 (1995).
9. M. Sugita, P. J. Peters, S. A. Porcelli, unpublished observations.
10. A. Aruffo and B. Seed, *J. Immunol.* **143**, 1723 (1989); S. P. Balk, P. A. Bleicher, C. Terhorst, *Proc. Natl. Acad. Sci. U.S.A.* **86**, 252 (1989).
11. I. V. Sandoval and O. Bakke, *Trends Cell Biol.* **4**, 292 (1994); F. Letourneur and R. D. Klausner, *Cell* **69**, 1143 (1992).
12. M. S. Marks *et al.*, *J. Cell Biol.* **131**, 351 (1995).
13. C. Harter and I. Mellman, *J. Cell Biol.* **117**, 311 (1992); J. S. Humphrey, P. J. Peters, L. C. Yuan, J. S. Bonifacio, *ibid.* **120**, 1123 (1993); S. Höning and W. Hunziker, *ibid.* **128**, 321 (1995); P. Voorhees *et al.*, *EMBO J.* **14**, 4961 (1995).
14. Complementary DNA for CD1b-TD was generated by polymerase chain reaction with the use of full-length CD1b cDNA (1) as a template DNA. The primers used were 5'-AGCGGATCCAGTGAACATGCTTCCAGGGG-3' (plus strand, 5' end of CD1b cDNA) and 5'-TCGGGATCCTAGCGCCTCATATACCATAA-3' (minus strand, 3' end). The amplified fragment was sequenced and subcloned into pSR $\alpha$ -neo for transfection into HeLa cells. The cytoplasmic amino acid sequences of CD1b-FL and CD1b-TD are Met-Arg-Arg-Arg-Ser-Tyr-Gln-Asn-Ile-Pro and Met-Arg-Arg, respectively.
15. M. A. Williams and M. Fukuda, *J. Cell Biol.* **111**, 955 (1990).
16. R. A. Rogers, R. M. Jack, S. T. Furlong, *J. Cell Sci.* **106**, 485 (1993).
17. H. Ohno *et al.*, *Science* **269**, 1872 (1995).
18. P. G. Lerch, M. van de Rijn, P. Schrier, C. Terhorst, *Hum. Immunol.* **6**, 13 (1983).
19. V. Lotteau *et al.*, *Nature* **348**, 600 (1990); O. Bakke and B. Dobberstein, *Cell* **63**, 707 (1990).
20. M. Sugita and M. B. Brenner, *J. Biol. Chem.* **270**, 1443 (1995).
21. D. Olive, P. Dubreuil, C. Mawas, *Immunogenetics* **20**, 253 (1984).
22. C1R cells with high expression of CD1b were obtained by supertransfection of CD1b-positive C1R cells (1) with CD1b cDNA in a hygromycin-resistant gene containing expression vector p3-9, followed by selection with hygromycin B (200  $\mu$ g/ml). The high-expressing cells were collected by fluorescence-activated cell sorting and used for immunoelectron microscopy analysis. Thin cryosectioning and immunogold labeling were carried out as described (5, 8), except for the use of the BCD1b3.1 antibody to CD1b [S. M. Behar, S. A. Porcelli, E. M. Beckman, M. B. Brenner, *J. Exp. Med.* **182**, 2007 (1995)] for detection of CD1b. Specificity of labeling with the antibody to CD1b was shown by the complete absence of labeling in mock-transfected (that is, CD1b<sup>-</sup>) C1R cells. For each immunolabeling, at least 2000 cells were evaluated.
23. L. K. Denzin, N. F. Robbins, C. Carboy-Newcomb, P. Cresswell, *Immunity* **1**, 595 (1994).
24. We thank H. Ploegh, J. Trowsdale, M. Fukuda, P. Cresswell, D. Olive, C. Mawas, V. Hsu, and W. Brown for their gifts of reagents; L. Glimcher of Harvard Medical School for the gift of expression vector p3-9; Genetics Institute (Cambridge, MA) for GM-CSF; Schering-Plough Corp. (Kenilworth, NJ) for IL-4; and V. Hsu for critically reading the manuscript. Supported by grants from NIH.

31 January 1996; accepted 13 April 1996

## Immunostimulatory DNA Sequences Necessary for Effective Intradermal Gene Immunization

Yukio Sato, Mark Roman, Helen Tighe, Delphine Lee, Maripat Corr, Minh-Duc Nguyen, Gregg J. Silverman, Martin Lotz, Dennis A. Carson, Eyal Raz\*

Vaccination with naked DNA elicits cellular and humoral immune responses that have a T helper cell type 1 bias. However, plasmid vectors expressing large amounts of gene product do not necessarily induce immune responses to the encoded antigens. Instead, the immunogenicity of plasmid DNA (pDNA) requires short immunostimulatory DNA sequences (ISS) that contain a CpG dinucleotide in a particular base context. Human monocytes transfected with pDNA or double-stranded oligonucleotides containing the ISS, but not those transfected with ISS-deficient pDNA or oligonucleotides, transcribed large amounts of interferon- $\alpha$ , interferon- $\beta$ , and interleukin-12. Although ISS are necessary for gene vaccination, they down-regulate gene expression and thus may interfere with gene replacement therapy by inducing proinflammatory cytokines.

Intramuscular (1) or intradermal (2) administration of pDNA expression vectors causes intracellular synthesis of the encoded proteins and induction of long-lasting cellular and humoral immune responses. Recently, we reported that mice injected or scratched intradermally with expression vectors encoding  $\beta$ -galactosidase ( $\beta$ -Gal) and containing a bacterial ampicillin resistance gene (*ampR*) produced a strong antibody response to  $\beta$ -Gal (3). However, subsequent experiments showed that mice injected intradermally with a similar expression vector containing the kanamycin resistance gene (*kanR*) instead of *ampR* generated a weak antibody response to  $\beta$ -Gal (Fig. 1 and Table 1). These results were unexpected, because we had always detected higher  $\beta$ -Gal activity in cells transfected with the *kanR*-based vector (pKCB) that encodes  $\beta$ -Gal, pKCB-Z (615.4 pg of  $\beta$ -Gal per well), than in cells transfected with the *ampR*-based vectors, pACB-Z and pACS-Z, encoding  $\beta$ -Gal (254.9 pg of  $\beta$ -Gal per well and 113.3 pg per well, respectively) (4).

To test the hypothesis that the *ampR* sequence may up-regulate the immune response to  $\beta$ -Gal in gene-vaccinated mice, we injected animals with pKCB-Z together with pDNA for either the *ampR* or *kanR* gene. The coadministration of pKCB-Z with vectors containing the *ampR* gene (pACB or pUC19) restored the antibody response to  $\beta$ -Gal to approximately the level induced by pACB-Z (Table 1). The immune stimulation was dose-related because coadministration of 100  $\mu$ g of pUC19 induced a larger specific antibody response than coadminis-

tration of 5  $\mu$ g of pUC19. In contrast, coadministration of pKCB-Z with the pKCB vector did not result in any significant enhancement of the antibody response to  $\beta$ -Gal (Table 1). The intradermal gene vaccination of mice with pKCB-Z did not induce a significant cytolytic T lymphocyte (CTL) response to  $\beta$ -Gal, as compared with the vigorous CTL response induced by pACB-Z (Fig. 2A). However, the coinjection of pKCB-Z with pACB or with pUC19 restored the CTL response to  $\beta$ -Gal to approximately the level observed in mice immunized with pACB-Z (Fig. 2A).

One of the main features of intradermal gene vaccination with naked pDNA is the induction of a T helper cell type 1 (T<sub>H</sub>1) response to the gene product (3, 5). This response is characterized by the production of a distinctive cytokine profile [interleukin-2 (IL-2), tumor necrosis factor- $\beta$  (TNF- $\beta$ ), and, mainly, interferon- $\gamma$  (IFN- $\gamma$ )] by antigen-stimulated CD4 T cells (6). The CD4 splenocytes from pACB-Z-immunized mice generated large amounts of IFN- $\gamma$  and small amounts of IL-4 (Fig. 2, C and D, respectively), whereas cells from pKCB-Z-immunized mice produced only trace amounts of these cytokines. However, the production of IFN- $\gamma$  could be restored in pKCB-Z-immunized mice by coinjection with the *ampR*-containing vectors, pACB and pUC19 (Fig. 2C).

Palindromic, single-stranded immunostimulatory DNA sequences (ISS) have been reported to induce production of IFN- $\alpha$ , IFN- $\beta$ , and IFN- $\gamma$  from mouse splenocytes and human peripheral lymphocytes and to enhance natural killer cell activity. These ISS include the following CpG-containing hexamers: 5'-GACGTC-3', 5'-AGCGCT-3', and 5'-AACGTT-3' (7). Two repeats of 5'-AACGTT-3' were in the *ampR*

Department of Medicine and The Sam and Rose Stein Institute for Research on Aging, University of California, San Diego, 9500 Gilman Drive, La Jolla, CA 92093-0663, USA.

\* To whom correspondence should be addressed.